

# Anhydrous Proton Conduction of Natural Aromatic Polymer: Preparation of Ligninsulfonic Acid-Heterocycle Composite and its Proton Conductivity

Masanori Yamada\* and Misaki Takeda

Department of Chemistry, Faculty of Science, Okayama University of Science, Ridaicho, Okayama 700-0005, Japan

\*E-mail: [myamada@chem.ous.ac.jp](mailto:myamada@chem.ous.ac.jp)

Received: 28 April 2018 / Accepted: 21 May 2018 / Published: 5 July 2018

---

Natural aromatic polymer ligninsulfonic acid (LS), which is a water-soluble acidic polymer, is a byproduct from the production of wood pulp using sulfite pulping. This material possesses a sulfonic acid group in its molecular structure. We demonstrated the utilization of LS as an anhydrous proton conductor. As a result, the LS showed the proton conductivity of  $1.8 \times 10^{-8} \text{ S cm}^{-1}$  at 180 °C under anhydrous conditions. The anhydrous proton conductivity increased with the composite of the heterocyclic molecule and reached the maximum value of  $9.1 \times 10^{-4} \text{ S cm}^{-1}$  at 80 mol% under similar conditions. The activation energy of the proton conduction was 0.2 – 1.4 eV which were one order of magnitude higher than that of the typical humidified perfluorinated membrane, and these values indicated the anhydrous proton conducting mechanism. The ligninsulfonic acid-heterocycle composite material may have the potential to be utilized as a novel proton conductor under anhydrous conditions.

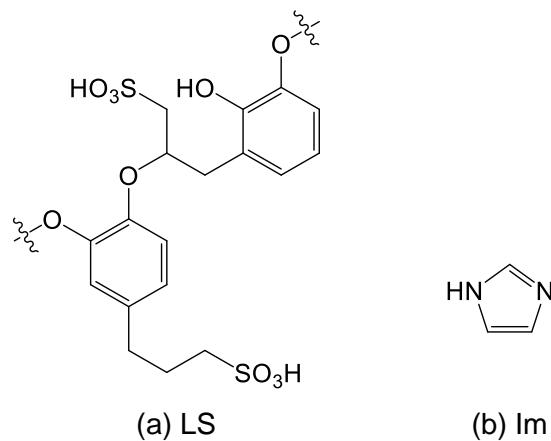
---

**Keywords:** Anhydrous proton conduction, Ligninsulfonic acid, Composite material, Energy material, Heterocyclic molecule

## 1. INTRODUCTION

Lignin, one of the most abundant natural aromatic polymers on the earth, is a class of complex organic polymers that form important structural materials in the support tissues of vascular plants [1-4]. Lignin is particularly important in the formation of cell walls, especially in wood and bark, because they lend rigidity and do not easily rot. Chemically, although lignins are cross-linked phenolic polymers, the detailed molecular structure has not been determined. These lignins are an unnecessary component in the industrial paper process and removed by a sulfite process [2]. The sulfite process produces the wood pulp which is almost pure cellulose fibers by using various salts of sulfurous acid to

extract the lignin from wood chips in high pressure vessels [2]. In this process, the byproduct is ligninsulfonic acid (LS), which is a water-soluble anionic polyelectrolyte polymer. Scheme 1 (a) shows the partial molecular structure of LS. The LS is used in tanning leather, making concrete, drilling mud, drywall, *etc.* However, many of these materials are considered industrial waste around the world [1,2]. Therefore, we demonstrated the novel utilization of LS for energy material as a proton conducting material. The development of lignin as an engineering material, such as a proton conductor, has not been reported to the best of our knowledge.



**Scheme 1.** (a) Partial molecular structure of ligninsulfonic acid (LS). (b) Molecular structure of imidazole (Im).

The proton conductor has been used as a sensor material, an ion selective electrode, and an actuator [5-7]. Especially, the anhydrous proton conductor is one of the most important components in the operation of a polymer electrolyte fuel cell at intermediate temperatures (100 - 200 °C) [8-11]. Generally, since the proton conduction of the typical humidified perfluorinated membrane is based on the presence of mobile water molecules in the membrane, the proton conductivity at >100 °C abruptly decreases due to the evaporation of the water from the membrane [8-11]. Therefore, an anhydrous proton conductor has been prepared based on a concept different from the conventional one. One of the concepts of the anhydrous proton conductor is an acid-base composite [8-11]. These anhydrous proton conductors were prepared by mixing acidic and basic heterocyclic molecules (or polymers). In this proton conducting mechanism, the acidic and heterocyclic molecules behave as a proton donor and acceptor, respectively, and the proton in the material can transfer from site to site without the assistance of diffusible vehicle molecules [12-14]. These acid-base composites typically consist of an expensive artificial polymer, which was synthesized from petroleum. Additionally, since these polymers are stable materials, they are difficult to discard after their use. In contrast, the LS is a material of natural origin and is biodegradable. Furthermore, the LS is one of the industrial wastes and is a low cost material. Therefore, the utilization of LS as a proton conducting material is a logical consideration.

In this study, we prepared a LS-heterocycle composite by mixing LS and a heterocycle, such as imidazole (Im). The LS-Im composite formed the acid-base complex, such as imidazolium organic salts. Additionally, the thermal stability of the LS-Im composite increased with the addition of Im. Furthermore, the anhydrous proton conductivity also increased with the addition of Im and reached the maximum value of  $9.1 \times 10^{-4} \text{ S cm}^{-1}$  at  $160 \text{ }^\circ\text{C}$  under anhydrous conditions. This value of the LS-Im composite was four orders higher than that of LS without the composite.

## 2. EXPERIMENTAL SECTIONS

### 2.1. Material

The sodium ligninsulfonate and imidazole (Im) were purchased from Tokyo Kasei Industries, Ltd., Tokyo, Japan, and Wako Pure Chemical Industries, Ltd., Osaka, Japan, respectively. Scheme 1 (b) shows the molecular structure of Im. The ion exchange resin Amberlite IR 120(H) was obtained from Supelco, Inc., Bellefonte, PA, USA. Solvents of an analytical grade were used in all the experiments. Ultra-pure water (Merck KGaA, Darmstadt, Germany) was used in this research.

### 2.2. Preparation of LS-Im composite

The sodium ligninsulfonate was changed from the  $\text{Na}^+$  form to  $\text{H}^+$  form by an ion exchange column containing an ion exchange resin [15]. The ion exchange of LS was confirmed by the pH measurement. The amount of sulfonic acid groups (the amount of  $\text{H}^+$ ) in the LS was estimated by titration and was  $3.3 \times 10^{-3} \text{ mol g}^{-1}$ . The molar ratio of the LS-Im composite was determined by Equation (1).

$$\text{mol\%} = \frac{[\text{Im}]}{[\text{LS}] + [\text{Im}]} \times 100 \quad (1)$$

where  $[\text{LS}]$  and  $[\text{Im}]$  are the molar concentration of LS (proton conversion) and Im, respectively. The molar ratio of LS-Im composite was changed at 0 mol% (LS without the composite), 30 mol%, 50 mol%, 70 mol%, 80 mol%, 90 mol%, and 100 mol% (Im without the composite). The LS-Im composite was prepared as follows: the aqueous LS-Im mixed-solution was prepared by the addition of Im (30 mol% - 90 mol%) to the aqueous LS solution ( $10 \text{ mg ml}^{-1}$ ). This mixed solution was incubated for 24 hours at RT, cast on a Teflon<sup>®</sup> plate, dried overnight at RT, then heated at  $80 \text{ }^\circ\text{C}$  for 1 hour. The LS without the composite and the Im without the composite was used for LS-0 mol% Im and LS-100 mol% Im composites, respectively.

### 2.3. Characterization of LS-Im composite

The infrared (IR) absorption spectra were measured by the attenuated total reflection (ATR) method with a diamond prism using an FT-IR 8400 Fourier transform infrared spectrometer (Shimadzu

Corp., Kyoto, Japan). The IR spectrum was measured with the resolution of  $4\text{ cm}^{-1}$ . The thermal stability of the LS-Im composite was analyzed using a DTG-60 thermogravimetric - differential thermal analyzer (TG-DTA) (Shimadzu Corp.). The TG-DTA measurement was carried out at the heating rate of  $10\text{ }^{\circ}\text{C min}^{-1}$  under a dry-nitrogen flow. Sample weights of the TG-DTA measurements were normalized at 1 mg.

### 2.5. Proton conductive measurement of LS-Im composite

The proton conductivity of the LS-Im composite was demonstrated by the a.c. impedance method in the frequency range from 4 Hz to 1 MHz using a chemical impedance analyzer 35320-80 (Hioki Co., Nagano, Japan) in a stainless steel vessel from RT to  $180\text{ }^{\circ}\text{C}$  under a dry-nitrogen flow [15,16]. The LS-Im composite was sandwiched between two gold electrodes (diameter: 5 mm) or two platinum electrodes (diameter: 6 mm) with a Teflon<sup>®</sup> spacer [15,16]. The direction of the conductive measurement was perpendicular to the composite. Before the measurements of the proton conduction, the composites were dried at  $180\text{ }^{\circ}\text{C}$  for 2 hours in a stainless steel vessel to evaporate the water and volatile components from the composite. Additionally, all the experimental procedures used for the proton conductive measurements were carried out under a dry-nitrogen flow. The conductivities of LS-Im composite materials were determined from Cole-Cole plots. The resistances of the composite materials were obtained by the extrapolation to the real axis.

## 3. RESULTS AND DISCUSSION

### 3.1. Molecular structure of LS-Im composite

The LS-Im composites were prepared by mixing LS and Im. The mixed solution of LS and Im was cast on a Teflon<sup>®</sup> plate and dried overnight at room temperature. The obtained LS-Im composites are brown films. The LS-Im composite films were analyzed by an IR spectrometer equipped with an ATR prism. Figure 1 shows the IR spectra of (a) LS without the composite, (b) LS-30 mol% Im composite, (c) LS-50 mol% Im composite, (d) LS-80 mol% Im composite, and (e) Im molecule without the composite. The LS without the composite showed adsorption bands at  $1024\text{ cm}^{-1}$  and  $1128\text{ cm}^{-1}$ , related to the asymmetric O=S=O stretching vibration and symmetric O=S=O stretching vibration, respectively [17-19]. The absorption band at  $1024\text{ cm}^{-1}$  shifted to a high wavenumber, ca.  $1010\text{ cm}^{-1}$ , with the addition of Im. Additionally, when the Im molecule was added to the LS, the absorption band at  $1128\text{ cm}^{-1}$  disappeared. These results suggested that the  $-\text{SO}_3\text{H}$  group in the LS became deprotonated by the addition of the basic Im molecule and formed the  $-\text{SO}_3^-$  group and the free proton. In contrast, the Im showed an absorption band at approximately  $3100\text{ cm}^{-1}$ , which corresponded to the stretching band of the N-H group [17,20]. When the Im molecules were added to the LS, the intensity of this adsorption band relatively increased in comparison to the pure Im molecule. Furthermore, the absorption band at  $1446\text{ cm}^{-1}$ , attributed to the aromatic C=N of the Im molecule [17,20], relatively decreased with the addition to the LS. This is due to the formation of N-H and collapse of the aromatic

C=N by the addition to the LS. These results suggested that the free proton from the LS interacts with the non-protonated  $-N=$  group of the Im molecule and forms the positively charged imidazole. Therefore, the LS-Im composite produced the acid-base salts, including the imidazolium organic salts. Similar phenomena have been reported for acid-base composites, such as the poly(vinylphosphonic acid)-heterocycle composite [21] and double-stranded DNA-Im composite [15].

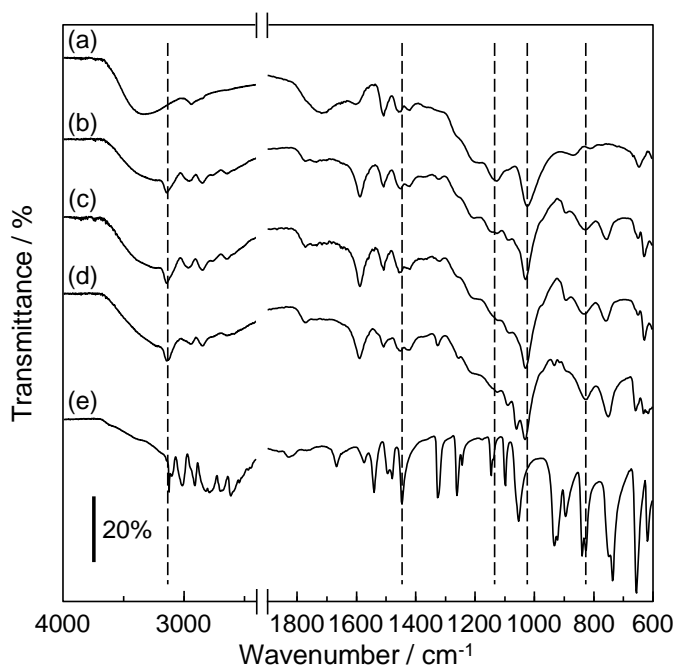


**Figure 1.** IR spectra of (a) LS without the composite, (b) LS-30 mol% Im composite, (c) LS-50 mol% Im composite, (d) LS-80 mol% Im composite, and (e) Im molecule. The IR spectrum was measured at the resolution of  $4\text{ cm}^{-1}$ . Triplicate experiments gave similar results.

### 3.2. Thermal stability of LS-Im composite

Figures 2 (a) and (b) show the thermogravimetric (TG) and differential thermal analyses (DTA) of (1) LS without the composite, (2) LS-30 mol% Im composite, (3) LS-50 mol% Im composite, (4) LS-70 mol% Im composite, (5) LS-80 mol% Im composite, (6) LS-90 mol% Im composite, and (7) Im molecule without the composite. The LS without the composite of Im (line (1) in Figure 2) showed the TG weight loss of approximately 10% at  $100\text{ }^{\circ}\text{C}$  and approximately 30% at  $200\text{ }^{\circ}\text{C}$ . The DTA curve showed an endothermic peak at  $124.6\text{ }^{\circ}\text{C}$ . Therefore, the TG weight losses at  $100\text{ }^{\circ}\text{C}$  and  $200\text{ }^{\circ}\text{C}$  are due to the evaporation of water and thermal decomposition, respectively. In contrast, the Im molecule without the composite of LS (line (7) in Figure 2) showed two endothermic peaks due to its melting and evaporation at  $89.6\text{ }^{\circ}\text{C}$  and  $137.1\text{ }^{\circ}\text{C}$ , respectively [15]. For the LS-Im composite (line (2) – (6) in Figure 2), the endothermic peak at  $90$ ,  $125$ , and  $137\text{ }^{\circ}\text{C}$  disappeared. Additionally, the TG weight loss of the LS-Im composite was  $< 10\%$  at  $150\text{ }^{\circ}\text{C}$ . These results suggested that the LS molecules are thermally stabilized by addition of the Im molecule. This thermal stabilization is due to the formation of the acid-base composite. Similar phenomena have been reported for acid-base composites [15,21].

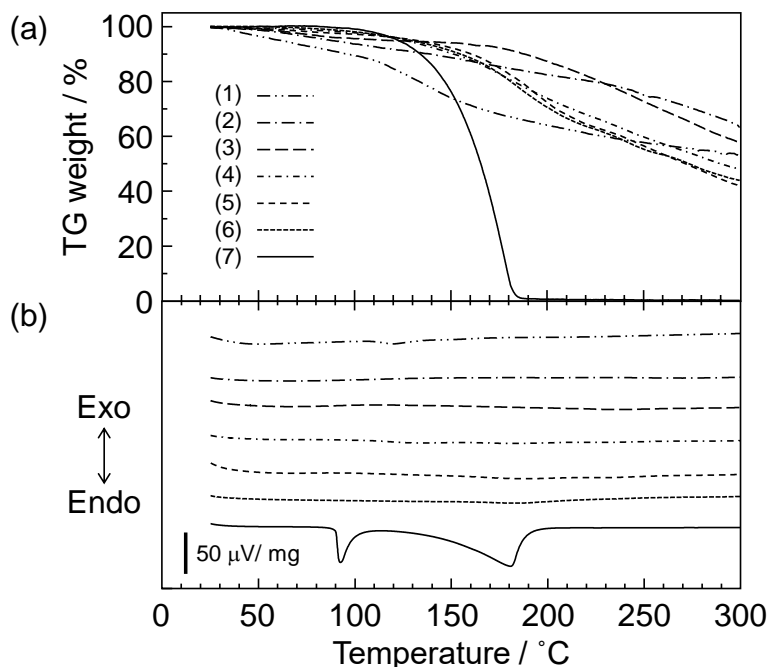


**Figure 2.** TG (a) and DTA (b) curves of (1) LS without the composite, (2) LS-30 mol% Im composite, (3) LS-50 mol% Im composite, (4) LS-70 mol% Im composite, (5) LS-80 mol% Im composite, (6) LS-90 mol% Im composite, and (7) Im molecule. These measurements were done at the heating rate of  $10\text{ }^{\circ}\text{C min}^{-1}$  under dry-nitrogen flow. Triplicate experiments gave similar results.

### 3.3. Anhydrous proton conduction of LS-Im composite

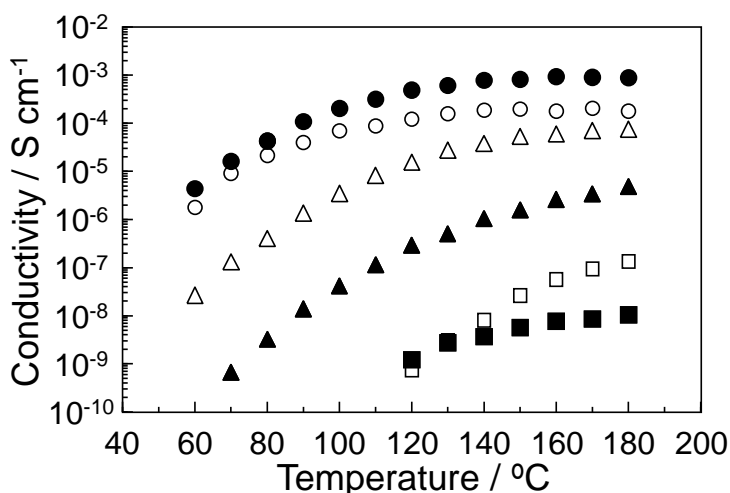


**Figure 3.** Proton conductivities of LS-Im composite under dry-nitrogen flow. (■) LS without the composite, (□) LS-30 mol% Im composite, (▲) LS-50 mol% Im composite, (△) LS-70 mol% Im composite, (●) LS-80 mol% Im composite, and (○) LS-90 mol% Im composite. The proton conductivity measurement was performed by the a.c. impedance method. These samples were dried at  $180\text{ }^{\circ}\text{C}$  for 2 hours under dry-nitrogen flow.

The proton conductivity measurements of the LS-Im composite were demonstrated by the a.c. impedance method under dry-nitrogen flow. The features of the Cole-Cole plots for the LS-Im

composite are similar to that of a highly-anhydrous proton conductor [15,16,21]. Additionally, according to the TG-DTA results (lines (1) – (6) in Figure 2), the diffusible ions other than the protons did not exist in these materials. Therefore, the impedance responses of the LS-Im composites are based on the anhydrous proton transfer without the assistance of diffusible vehicle molecules.

Figure 3 shows the proton conduction of (■) LS without the composite, (□) LS-30 mol% Im composite, (▲) LS-50 mol% Im composite, (△) LS-70 mol% Im composite, (●) LS-80 mol% Im composite, and (○) LS-90 mol% Im composite. The proton conduction of the LS-Im composite increased with the temperature and reached a maximum value at 160 °C or 180 °C. Figure 4 shows the maximum proton conductivity of the LS-Im composite. The LS without the composite showed the proton conductivity of  $1.8 \times 10^{-8} \text{ S cm}^{-1}$ . The proton conductivity of LS increased with the addition of the Im molecule, indicated the maximum proton conductivity at 80 mol%, then decreased at  $\geq 90$  mol%. The value of the maximum proton conductivity at 80 mol% was  $9.1 \times 10^{-4} \text{ S cm}^{-1}$  and was four orders of magnitude higher than that of the LS without the composite. In contrast, the Im molecules without the composite did not indicate proton conduction due to their evaporation during the heat treatment process at 180°C for 2 hours.

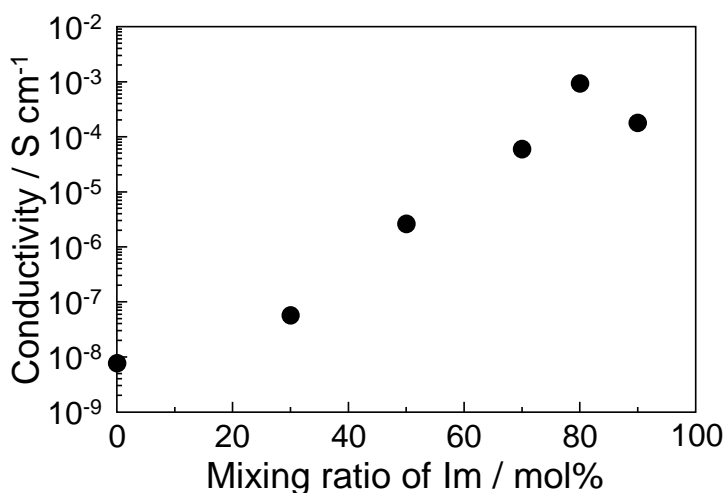


**Figure 4.** The maximum proton conductivity of the LS-Im composite. The proton conductive measurements were done under a dry-nitrogen flow.

Figure 5 shows the Arrhenius plots of the proton conduction of (■) LS without the composite, (□) LS-30 mol% Im composite, (▲) LS-50 mol% Im composite, (△) LS-70 mol% Im composite, (●) LS-80 mol% Im composite, and (○) LS-90 mol% Im composite. Since the Arrhenius plots of the LS-Im composite showed a straight line, the proton conduction of each composite is related to a single proton conducting mechanism. The activation energy ( $E_a$ ) of the proton conduction was calculated from the slope of the straight line. Table 1 shows the  $E_a$  of the proton conduction in LS-Im composite. Although the  $E_a$  values abruptly increased by the addition of Im to the LS (see 30 mol% in Table 1), these values then decreased with the addition of the Im molecules. These  $E_a$  values are one order of magnitude higher than that of the typical humidified perfluorinated membranes [22,23]. Similar  $E_a$

values have been reported for the poly(vinylphosphonic acid)-heterocycle composite [21] and double-stranded DNA-Im composite [15]. These results suggested that the proton conduction of the LS-Im composite is based on the anhydrous proton conducting mechanism without the assistance of diffusible water molecules.

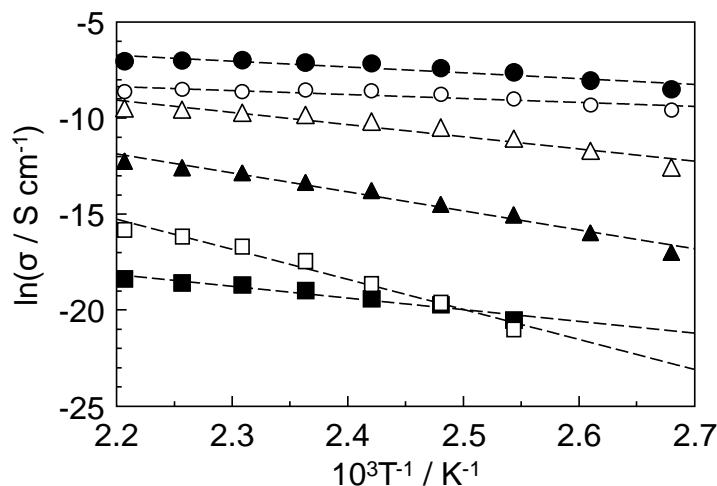


**Figure 5.** Arrhenius plots of the proton conductivity of the LS-Im composite. The solid lines are the results of a least-squares fitting. (■) LS without the composite, (□) LS-30 mol% Im composite, (▲) LS-50 mol% Im composite, (△) LS-70 mol% Im composite, (●) LS-80 mol% Im composite, and (○) LS-90 mol% Im composite.

**Table 1.** The activation energy ( $E_a$ ) of proton conduction in the LS-Im composite.

Mixing ratio of Im	$E_a$ / eV
LS-0 mol% Im (LS)	0.52
LS-30 mol% Im	1.35
LS-50 mol% Im	0.85
LS-70 mol% Im	0.55
LS-80 mol% Im	0.26
LS-90 mol% Im	0.18

We previously reported a proton conducting acid-base composite membrane with the heterocyclic molecule under anhydrous conditions [15,21]. In this case, a Grotthuss-type mechanism was proposed, in which the transport of the proton in basic heterocyclic molecules can occur from protonated molecules to non-protonated neighboring molecules with the low  $E_a$  of approximately 0.2 eV [12,15,21,24]. In this investigation, since the proton conduction of the LS without the composite of the Im molecule is based on the proton transfer between the sulfonic acids, the value of  $E_a$  in the LS was higher than that of other reported values [12,15,21,24]. The amount of sulfonic acid by titration was  $3.3 \times 10^{-3} \text{ mol g}^{-1}$  and the distance between the sulfonic acids groups is too long to transfer the proton. As a result, the  $E_a$  of the LS was higher than the reported  $E_a$ . For the LS-30 mol% Im



composite, the sulfonic acid group and Im molecules form the acid-base composite. As a result, the number of free protons to transfer to neighboring sites decreased and the value of  $E_a$  became higher. For the  $\geq 50$  mol% Im composite, the Im molecules in the LS-Im composite formed a proton conducting pathway. Generally, the Im molecules have been reported to form a molecular cluster consisting of approximately twenty molecules through intermolecular hydrogen bonding [25]. As a result, this anhydrous proton conduction has occurred from the protonated Im molecules to the non-protonated neighboring Im molecules and the value of  $E_a$  decreased with the addition of the Im molecule. The obtained  $E_a$  for the LS-80 mol% Im composite was almost the same as that reported for the acid-Im composite material [15,21].

#### 4. CONCLUSION

We prepared the LS-Im composite by mixing ligninsulfonic acid (LS) and the heterocycle imidazole (Im). The LS and Im formed an acid-base composite by an interaction between the sulfonic acid group and non-protonated  $-N=$  site in the Im molecule. Additionally, the thermal stability of the LS-Im composite increased with the formation of the acid-base composite. Furthermore, the LS without the composite of Im showed a low proton conductivity on the order of  $10^{-8}$  S  $\text{cm}^{-1}$  at 180 °C under anhydrous conditions, however, the proton conductivity increased with the addition of Im and indicated the maximum value of  $9.1 \times 10^{-4}$  S  $\text{cm}^{-1}$  for the LS-80 mol% Im composite under similar conditions. The proton conducting biopolymers, consisting of industrial waste, have the potential to be utilized for applications in an implantable battery, bio-sensors, actuators, *etc.*

#### References

1. E.E. Harris, *Ind. Eng. Chem.*, 32 (1940) 1049.
2. F.E. Brauns, D.A. Brauns, *The chemistry of lignin*, Academic press, (1960) New York, USA.
3. D. Kai, M.J. Tan, P.L. Chee, Y.K. Chua, Y.L. Yap, X.J. Loh, *Green Chem.*, 18 (2016) 1175.
4. E. Adler, *Wood Sci. Technol.*, 11 (1977) 169.
5. H. Gao, K. Lian, *RSC Adv.*, 4 (2014) 33091.
6. L. Cao, X. He, Z. Jiang, X. Li, Y. Li, Y. Ren, L. Yang, H. Wu, *Chem. Soc. Rev.*, 46 (2017) 6725.
7. K.D. Kreuer, *Chem. Mater.*, 26 (2014) 361.
8. M. Rikukawa, K. Sanui, *Prog. Polym. Sci.*, 25 (2000) 1463.
9. J.A. Asensio, E.M. Sánchez, P. Gómez-Romero, *Chem. Soc. Rev.*, 39 (2010) 3210.
10. J. Peron, Z. Shi, S. Holdcroft, *Energy Environ. Sci.*, 4 (2011) 1575.
11. A.C. Dupuis, *Prog. Mater. Sci.*, 56 (2011) 289.
12. K.D. Kreuer, *Chem. Mater.*, 8 (1996) 610.
13. S.Ü. Çelik, A. Bozkurta, S.S. Hosseini, *Prog. Polym. Sci.*, 37 (2012) 1265.
14. I. Honma, M. Yamada, *Bull. Chem. Soc. Jpn.*, 80 (2007) 2110.
15. M. Yamada, A. Goto, *Polym. J.*, 44 (2012) 415.
16. M. Yamada, Y. Moritani, *Electrochim. Acta*, 144 (2014) 168.
17. R.M. Silverstein, F.X. Webster, *Spectrometric Identification of Organic Compounds*, John Wiley & Sons, (1998) New York, USA.

18. A. Nersasian, P.R. Johnson, *J. Appl. Polym. Sci.*, 9 (1965) 1653.
19. W. Chen, J. A. Sauer, M. Hara, *Polymers*, 45 (2004) 7219.
20. M. Kawahara, J. Morita, M. Rikukawa, K. Sanui, N. Ogata, *Electrochim. Acta*, 45 (2000) 1395.
21. M. Yamada, I. Honma, *Polymer*, 46 (2005) 2986.
22. Y. Sone, P. Ekdunge, D. Simonsson, *J. Electrochem. Soc.*, 143 (1996) 1254.
23. J.D. Kim, I. Honma, *J. Electrochem. Soc.*, 151 (2004) A1396.
24. H. Kato, T. Kasuga, *Mater. Lett.*, 79 (2012) 109.
25. R.M. Acheson, *An Introduction to the Chemistry of Heterocyclic Compounds*, 3rd ed., John Wiley & Son, (1976) New York, USA.

© 2018 The Authors. Published by ESG ([www.electrochemsci.org](http://www.electrochemsci.org)). This article is an open access article distributed under the terms and conditions of the Creative Commons Attribution license (<http://creativecommons.org/licenses/by/4.0/>).